crystals

MDPI

Article

WAXS and SAXS Investigation of Collagen-Rich Diet Effect on Multiscale Arrangement of Type I Collagen in Tilapia Skin Fed in Aquaponics Plant

Alberta Terzi [1], Teresa Sibillano [1,*], Liberato De Caro [1], Davide Altamura [1], Nunzia Gallo [2], Maria Lucia Natali [2,3], Alessandro Sannino [2], Luca Salvatore [2,3], Federica Stella Blasi [2], Angelo Corallo [2] and Cinzia Giannini [1]

[1] Institute of Crystallography National Research Council, 70125 Bari, Italy; alberta.terzi@ic.cnr.it (A.T.); liberato.decaro@ic.cnr.it (L.D.C.); davide.altamura@ic.cnr.it (D.A.); cinzia.giannini@ic.cnr.it (C.G.)
[2] Department of Engineering for Innovation, University of Salento, 73100 Lecce, Italy; nunzia.gallo@unisalento.it (N.G.); marialucia.natali@unisalento.it (M.L.N.); alessandro.sannino@unisalento.it (A.S.); luca.salvatore@unisalento.it (L.S.); federicastella.blasi@unisalento.it (F.S.B.); angelo.corallo@unisalento.it (A.C.)
[3] Typeone Biomaterials S.r.l. di Muro Leccese, 73036 Lecce, Italy
* Correspondence: teresa.sibillano@ic.cnr.it

Abstract: Type I collagen is the main component of the extracellular matrix that acts as the physical and biochemical support of tissues. Thanks to its characteristics, collagen is widely employed as a biomaterial for implantable device fabrication and as antiaging food supplementation. Because of the BSE transmission in the 1990s, aquatic animals have become a more suitable extraction source than warm-blooded animals. Moreover, as recently demonstrated, a supplementing diet with fish collagen can increase the body's collagen biosynthesis. In this context, Tilapia feeding was supplemented with hydrolyzed collagen in order to enhance the yield of extracted collagen. Tilapia skin was investigated with wide and small angle scattering techniques, analyzing the collagen structure from the submolecular to the nanoscale and correlated with Differential Scanning Calorimetry (DSC) measurements. Our studies demonstrated that the supplementation appears to have an effect at the nanoscale in which fibrils appear more randomly oriented than in fish fed with no supplemented feed. Conversely, no effect of a collagen-rich diet was observed at the submolecular scale.

Keywords: type I collagen; WAXS; SAXS; Tilapia skin; dietary supplementation

Citation: Terzi, A.; Sibillano, T.; De Caro, L.; Altamura, D.; Gallo, N.; Natali, M.L.; Sannino, A.; Salvatore, L.; Blasi, F.S.; Corallo, A.; et al. WAXS and SAXS Investigation of Collagen-Rich Diet Effect on Multiscale Arrangement of Type I Collagen in Tilapia Skin Fed in Aquaponics Plant. *Crystals* **2022**, *12*, 700. https://doi.org/10.3390/cryst12050700

Academic Editor: Borislav Angelov

Received: 26 March 2022
Accepted: 11 May 2022
Published: 14 May 2022

1. Introduction

Type I collagen is the main fibrous protein of the mammalian body (about 70% of the overall collagen in mammals) [1]. Because of its peculiar hierarchical structure and its peptide composition, it is widely used for several applications in the biomedical field. It is composed of triple helices made up of two α1 (I) helices and one α2 (II) helix twisted in a trimeric molecule measuring 1.5 nm in diameter and about 300 nm in length [2]. The helical portion of the collagen molecule is characterized by the strict repetition of the Gly–X–Y triplet in which Pro and Hyp are often placed in the X and Y positions and glycine in every third position, guaranteeing the stabilization of the molecule, together with water molecules that assure the formation of hydrogen bonds around the triple helices. Collagen molecules are packed in a supramolecular arrangement called fibril, with a lateral packing distance of about 1.6 nm that varies in relation to the specific tissue and to the hydration. Within the fibril, along its axis, each collagen molecule is staggered about one quarter of its length with respect to the closest molecule [3]. This peculiar organization leads to alternating zones of low and high electron density distribution, which have been investigated several times [4,5] and named "D-banding" of about 64–67 nm of axial periodicity and are related to the gap-overlap triple helices zones within the fibril. Finally, fibrils are packed in fiber

and the fibers in bundles. The collagen deposition within tissues is strongly correlated to the forces acting on it, to the stresses it undergoes, and to the final function of the tissue [6]. For this reason, in tendons, fibrils, fibers, and bundles of collagen run parallel to the length of the tissue, as the matrix has to support uniaxial forces that act along the tendon length. [4,7,8] Conversely in skin, mainly in the dermis, collagen fibrils and fibers (from 3 to 40 µm in diameter) are mainly randomly organized in a loose network that supports multidirectional forces [9]. As it is responsible for the strength, stiffness, and stability of the extracellular matrix (ECM) in tissues, type I collagen is the gold standard natural biomaterial employed for the fabrication of implantable devices in regenerative medicine. Indeed, thanks to its biocompatibility, fibroblasts recognize the scaffold and are able to attach to it in wounds. Furthermore, during the regeneration processes, the collagenous matrix, which is degraded by enzymes and peptides, becomes useful for the new matrix building. Type I collagen is not only an excellent biomaterial, but it is also employed in both fibrillary and hydrolyzed forms in the cosmetic, food, and nutraceutical sectors and as dietary supplements for its ability to contribute to the viscoelasticity maintenance of soft tissues, such as the dermal layer of skin [10] and joints. Laying in connectives, it retains the hydration and the overall healthy conditions of the body. The sources commonly employed for collagen extraction are both terrestrial and marine animals, but most of the commercially available collagen is typically extracted from warm-blooded animals, such as bovines, horses, and pigs [6,11]. Collagens from warm-blooded animals possess a higher content of proline and hydroxyproline and a higher denaturation temperature (25–30 °C) compared to collagens from fish that make it more suitable for biomedical applications [4]. However, after several zoonotic pathologies emerged in recent decades, such as BSE (Bovine Spongiform Encephalopathy), more interest was placed on marine sources of collagen [11], which are less stable but considered GRAS (generally considered as safe) by the Federal Drugs Administration (FDA). Of note, 75% of the fish weight is composed of collagen, particularly scales, fins, bones, and skin [12] and tissues that are generally considered waste during industrial fish processing. Recycling them as collagen sources allows us to obtain commercial products with a high benefit as part of a green economy project, helping to solve the problem of waste disposal and the loss of important biological substances and to reduce the cost of the final product. An important issue of marine sources is the collagen yield. In fact, mammalian sources allow access to a larger amount of extraction tissues than fish sources. In recent years, several preclinical studies showed how oral collagen peptide supplementation can improve the deposition of collagen, in particular "coarse collagen", in human skin, [13–15] better than the topical application of collagen-rich cosmetics [16]. However, there are no studies about collagen deposition and organization in animals fed with hydrolyzed collagen supplementation. In this context, with the final aim to increase the collagen content of Tilapia skin, we attempted to stimulate collagen production directly by supplementing the animal feed with hydrolyzed collagen. The addition of peptides or hydrolyzed collagen to conventional feed leads to the modulation of tissue structure and function directly from the inside contributing to its homeostasis [17]. To the best of our knowledge, this is the first study about the effect of hydrolyzed collagen supplementation on the hierarchical arrangement of fish skin collagen over time. In fact, while the modification of the collagen structure due to the age was investigated [13,18], less is known about the multiscale structural effect of collagen supplementation on the hierarchical arrangement of type I collagen during aging. Thus, with the aim to investigate the effect of the oral hydrolyzed collagen supplementation on the structural features of type I collagen in the skin of Tilapia fish grown in an aquaponics plant, wide and small angle X-ray scattering (WAXS and SAXS) measurements and Differential Scanning Calorimetry (DSC) were performed, and data were collected from pieces of skin taken from animals of the aquaponic plant.

2. Materials and Methods

Type I collagen investigations were performed on skin pieces of Nile Tilapia (*Oreochromis niloticus*) bred in the aquaponics plant of the "Urban Farming Lab" of the Department of Innovation Engineering (University of Salento, Lecce, Italy). The fish were fed with conventional feed (EFICO Cromis 832F 3, BioMar, Nersac, France) and 3% (*w*/*w*) hydrolyzed collagen-supplemented feed (hydrolyzed type I collagen from equine tendon, Typeone Biomaterials Srl, Lecce, Italy). Skin samples from animals were taken at different time points, particularly at 0, 2, and 4 months of feeding. Nonfish skin components (i.e., scales and fillet) were immediately eliminated with a knife. Then, fish skins were rinsed three times with distilled water and stored at −20 °C in a polyethylene bag. Prior to use, samples were thawed at 4 °C. Samples from fish of different ages and fed with and without collagen supplementation are listed in Table 1.

Table 1. Fish skins from animals fed with and without collagen-rich feed (supplementation) for 0, 2, and 4 months are listed.

	0 Month	2 Months	4 Months
no collagen-rich diet	TG_0M	TG_2M_CTRL	TG_4M_CTRL
collagen-rich diet	/	TG_2M_TRAT	TG_4M_TRAT

Wide (WAXS) and small (SAXS) angle X-ray scattering measurements were performed at the X-ray Micro Imaging Laboratory (XMI-L@B) [19]. WAXS and SAXS data were collected by an experimental setup in which the Fr-E+ SuperBright copper anode MicroSource (λ = 0.154 nm, 2475 W) was coupled through a focusing multilayer optics Confocal MaxFlux (CMF 15–105) to a three-pinhole camera for X-ray measurements for both WAXS and SAXS data collection. The beam size at the sample was about 0.3 × 0.3 mm^2.

Slices of fish skin of about 0.37 ± 0.12 mm thick were kept in Ultralene® sachets together with a drop of distilled water for X-ray acquisition. The sachets were then sealed in order to preserve the hydration state of the tissues. Ultralene® is a thin film that confers the uniform transmission of X-rays. Because of its chemical and heat strength and good X-ray transmission, it is commonly used in X-ray analysis with liquid and wet samples. The sealed sachets of Ultralene® with the fish skins were mounted on a sample holder and placed in a chamber in vacuum (0.1/1 mbar) during acquisition. WAXS data were acquired by an Image Plate (IP) detector (250 × 160 mm^2, 100 μm effective pixel size) placed at a ~10 cm distance from the sample in order to collect data in a range of 1.8/21 Å in the direct space (0.3 to 3.5 $Å^{-1}$ in the reciprocal space). For SAXS measurements, data were collected in a range of 3/60 nm in the direct space (0.01 to 0.2 $Å^{-1}$ in the reciprocal space), placing the IP detector at a ~1.5 m distance from the sample. The WAXS and SAXS measurements were digitally extracted by an off-line RAXIA reader. WAXS and SAXS data were elaborated by SAXSGUI and SUNBIM [20] software.

Detector–sample distances were calibrated by using the powder of the SiNist standard sample for WAXS and the powder of the AgBen standard sample, both placed in Ultralene® sachets. The experimental plan was composed of three different ages and two different feed conditions; thus, five samples are listed in Table 1, and three WAXS signals from three different areas of the same sample for each condition were acquired. Each point was acquired for 1200 s for a total time of 3600 s for each condition of the experimental plan.

DSC measurements were performed using a Q2000 Series DSC from TA Instruments (New Castle, DE, USA). Dry skin samples were accurately weighed (5–10 mg) into aluminum pans, hermetically sealed, and scanned from 5 °C to 100 °C at 5 °C/min in inert nitrogen atmosphere (50 mL min^{-1}) [21,22]. An empty aluminum pan was used as a reference probe. The temperature at which the endothermic phenomenon occurred was measured as the mid-point of the corresponding endothermic peak [22,23]. The area under the peak was calculated to estimate the enthalpy required for the transition [22,23]. The obtained data were analyzed using the OriginPro software (Origin-Lab version 8,

Northampton, MA, USA). Three fish skin pieces belonging to three different fish specimens were tested for each sample type. Each fish skin piece was run in triplicate as for X-ray acquisition, as described in the following.

3. Results and Discussion

3.1. Wide Angle X-ray Scattering Analysis

For the investigation of the type I collagen arrangement at molecular scale, WAXS measurements were performed. Indeed, by exploiting the interference pattern of the secondary waves scattered by the atomic electron density distribution of the fibrous protein, it was possible to investigate the molecular structure of the collagen.

Figure 1a shows the 2D WAXS pattern collected on Tilapia skin from the control fish TG_0M. As known from the literature, collagen triple helices assemble into fibrils with a variable lateral packing distance in a q range of q = 0.35–0.50 $Å^{-1}$, corresponding to a distance d of 12–18 Å (typical distance along the equatorial direction).

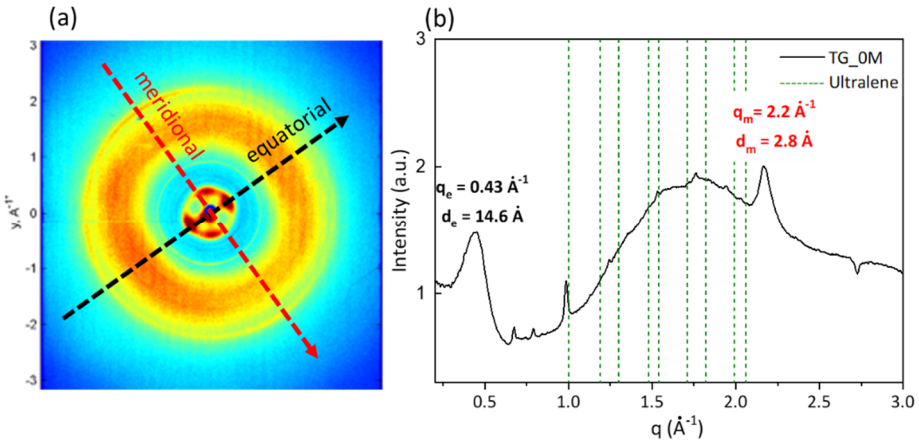

Figure 1. Two-dimensional WAXS diffraction pattern of Tilapia skin from the control fish (**a**) shows the equatorial (black arrow) and meridional (red arrow) directions identified by the peak positions in the corresponding (**b**) 1D diffraction pattern. Vertical dotted bars refer to Ultralene® sachet diffraction. (See Figure S3 in the Supplementary Materials).

Here, the fish skin exhibits the typical diffraction signals whose intensity is anisotropically distributed along the equatorial direction (marked by the black arrow in Figure 1a), i.e., perpendicular to the fiber axis and related to the lateral packing of collagen molecules. Otherwise, the intensity along the meridional direction (marked by the red arrow in Figure 1a), i.e., along the fiber axis, is characterized by a ring with an almost uniform intensity along the azimuth. This signal is a marker of the distance between two adjacent amino acids along the central axis of the triple helix of collagen. Both of them are related to the crystalline structural component of type I collagen [24–27].

Here, the equatorial diffraction signal in fish skin shows a characteristic pattern with a "four-lobe" shape. This is a noteworthy difference to what was previously observed on equine tendons [3,28] in which the typical fiber diffraction density distribution is localized along the equator direction, with a "two-lobe" shape. The geometry of the equatorial signal is still under investigation. However, one of the hypotheses is that the four-lobe signal is the overlap of two layers of fibers tilted one to the other.

One-dimensional diffraction profiles were analyzed by integrating the diffraction pattern along the entire azimuth. In Figure 1b, the equatorial peak, located at about $q_e = 0.42 \pm 0.02$ $Å^{-1}$ ($d_e = 14.60 \pm 0.83$ Å) and the meridional peak, located at about $q_m = 2.2$ $Å^{-1} \pm 0.2$ $Å^{-1}$ ($d_m = 2.8$ Å ± 0.5 $Å^{-1}$), allowed us to identify the Rich Crick molecular model [29] of a 10/3 helix (with a pitch length of 86 Å and the smallest axial periodicity of 2.8 Å). An additional broad peak between them is marked in a q range of 0.8–2.1 $Å^{-1}$ (d = 2.9–7.8 Å) and represents the amorphous component of collagen, which

was attributed to the distance between collagen skeletons [30]. Some peaks below q = 1 $Å^{-1}$ were due to some impurities present on the skin surface.

The visual inspection of the fish skin shreds showed that the white portion of the skin was wider in the samples with a collagen-rich diet (Pictures in Figure 2d,e) compared to the controls (Pictures in Figure 2a–c). This could probably be due to the increase in the ECM deposition after feeding, made of collagenous scaffold in noncollagenous molecules, in the skin tissue, also commonly found in skin pigmentation due to chromatophores and/or pigment cells, such as melanophores and xantophores. However, the enhanced ECM decreases the pigmentation of the tissue [23].

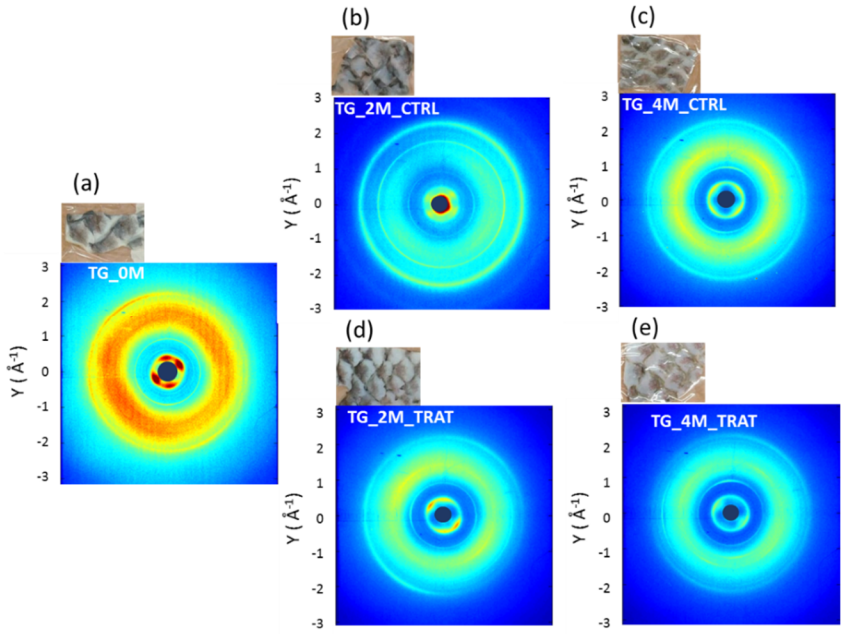

Figure 2. Pictures and 2D WAXS diffraction patterns of Tilapia skin from (**a**) the control fish at time point 0 (TG_0M), fish fed for (**b**) two months (TG_2M_CTRL), and (**c**) four months (TG_4M_CTRL) with conventional feed, fish fed for (**d**) two months (TG_2M_TRAT), and (**e**) four months (TG_4M_TRAT) with collagen nutritional supplementation.

Figure 2 shows the 2D WAXS patterns collected on Tilapia skin extracted from the control fish TG_0M (Figure 2a), the fish fed with conventional feed for two (TG_2M_CTRL) (Figure 2b) and four months (TG_4M_CTRL) (Figure 2c) and the fish fed with collagen-rich feed for two (TG_2M_TRAT) (Figure 2d) and four months (TG_4M_TRAT) (Figure 2e). Regarding the equatorial diffraction marker of the lateral packing of the collagen molecules, the control sample shows a peculiar diffraction intensity distribution with the maximum intensity distribution in four directions (preferred orientation), a "four-lobe" signal. As shown below, this peculiar intensity distribution changes when fish were fed with collagen supplementation.

Thus, the aforementioned "four-lobe"-shaped signal is clearly detected in TG_0M (Figure 1a) and TG_2M_CTRL (Figure 1b), while in the other samples, this characteristic intensity distribution appears different. The four lobes are no longer clearly distinguishable, but the intensity appears more uniformly distributed along a specific direction, forming arc-shaped signals, in particular, for the samples TG_2M_TRAT (Figure 2d), TG_4M_CTRL (Figure 2c), and TG_4M_TRAT (Figure 2d). This is an indication of a less oriented distribution of the molecules in the layers in the illuminated volume of the specimen.

After integrating the diffraction patterns in 1D WAXS profiles, only the equatorial peak was analyzed. In particular, radial integration along the equatorial direction allowed us to obtain 1D WAXS profiles (Figure 3a,b) that were the sum of three repeats acquired for each experimental condition. As shown in Figure 3a, the equatorial reflections of the control fish skin obtained from fish fed for 2 months (TG_2M_CTRL, red profile) and 4 months

(TG_4M_CTRL, blue profile) were shifted at q = 0.52 ± 0.05 Å^{-1} d = 12.08 ± 0.65 Å with respect to the equatorial peak position of the control sample at time point 0 (TG_0M) at q = 0.43 ± 0.03 Å^{-1} d = 14.61 ± 1.1 Å. This reflects the reduction of the lateral distance between molecules (triple helices) in the lateral arrangement of collagen. The fact that the shift is also observed in Figure 3b (displaying a comparison between T0 (black profile) and in skin from fish with a collagen-rich diet T2_TRAT (red profile) and T4_TRAT (blue profile)) suggests that the tighter packing of collagen triple helices could be connected to the growth of the age of the animal that leads to increased collagen deposition and decreased hydration of the fibrous protein, rather than dietary supplementation.

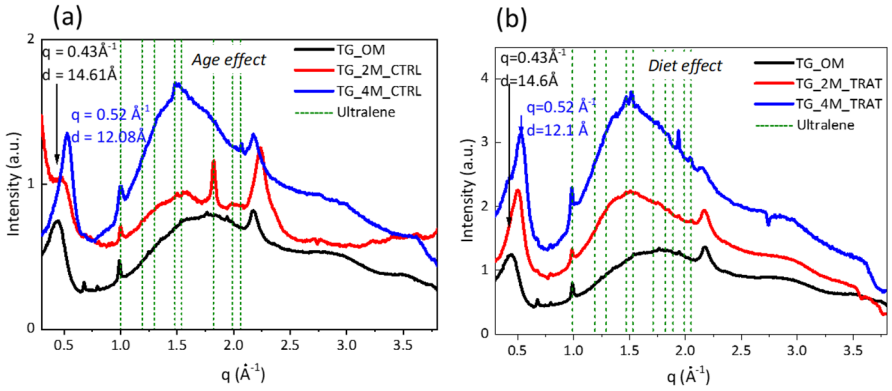

Figure 3. One-dimensional WAXS diffraction profiles obtained from radial integration of the signal selecting the q range of the equatorial signal (red dotted panel) of Tilapia skin. The comparison is shown between 1D profiles of fish fed with conventional feed (**a**) at time point 0 (TG_0, black profile) and after two and four months of diet (TG_2M_CTRL, red profile and TG_4M_CTRL, blue profile) and fish fed with conventional feed (**b**) at time point 0 (T0, black profile) and fish fed with a collage-rich diet for two and four months (TG_2M_TRAT, red profile and TG_4_M_TRAT, blue profile).

Additionally, it is worth noting that the meridional diffraction signal was also investigated (data not reported), even if it was slightly visible in the 2D patterns. Its value, obtained by the radial integration in 1D profiles, was the same in all samples (d = 2.8 ± 0.1 Å).

3.2. Small Angle X-ray Scattering Analysis

In order to investigate the supramolecular organization of the tissues, regarding the fibrillary arrangement of type I collagen at nanoscale, SAXS measurements were performed.

As shown in Figure 4, starting from TG_0 (a), passing through TG_2M_CTRL (b) to TG_4M_CTRL (c), the electron density distribution become more intense along a specific meridional direction (Figure 4c, red arrow); thus, more molecules had the same orientation in the tissue space that justifies the more oriented signal with the age of the animal. In addition, the Tilapia skin fed for 4 months with conventional feed (TG_4M_CTRL) revealed a higher preferential orientation (Figure 4c, red arrow) of the fibrils along their axis unlike the T0 (a) and TG_2M_CTRL (b) samples and a fiber-like shape (Figure 4c, red circle). This more structured organization of collagenous fibers could be ascribed to aging, that leads to a more mature and tight arrangement of the fibrous protein. When the animal is fed a collagen-rich supplementation (Figure 4e), the aforementioned features are not visible. On the contrary, it seems that the diet rich in collagen leads to the loss of preferential orientation of the diffraction signal and thus of the fibrils along their axis, and the fiber-like shape is no longer visible.

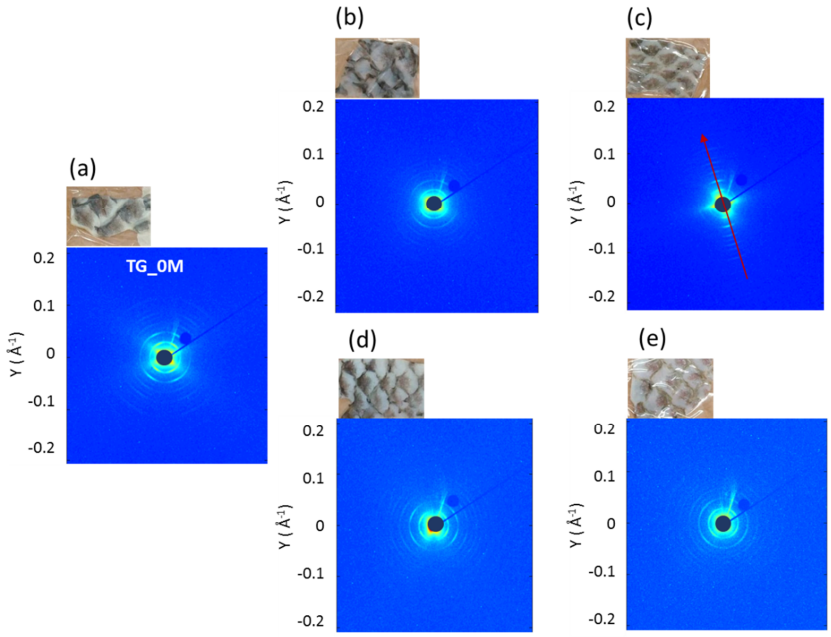

Figure 4. Two-dimensional SAXS diffraction patterns of Tilapia skin from (**a**) the control fish at time point 0 (TG_0M), fish fed for (**b**) two months (TG_2M_CTRL), and (**c**) four months (TG_4M_CTRL) with conventional feed; fish fed for (**d**) two months (TG_2M_TRAT) and (**e**) four months (TG_4M_TRAT) with collagen nutritional supplementation. (**c**) The red arrow shows the meridional direction, the fiber axis, and the red circle marks the fiber-like diffraction signal.

Despite this, the typical electron density distribution along the collagen fibrils that gives rise to the SAXS diffraction pattern with a series of 66 ± 2 nm-spaced fringes is observed in fish skin of fish fed a conventional diet (Figure 5, black profile). A slight difference in fibril spacing is visible in the fish skin of fish fed a collagen-rich diet (d-spacing = 65 nm ± 2 nm), showing that the fibril spacing coincides within the estimated errors. This evidence highlights that despite the fact that the fibrils are randomly oriented in the space, the fibrillary banding given by the molecular gap-overlap zones within the nanometric structure is still present.

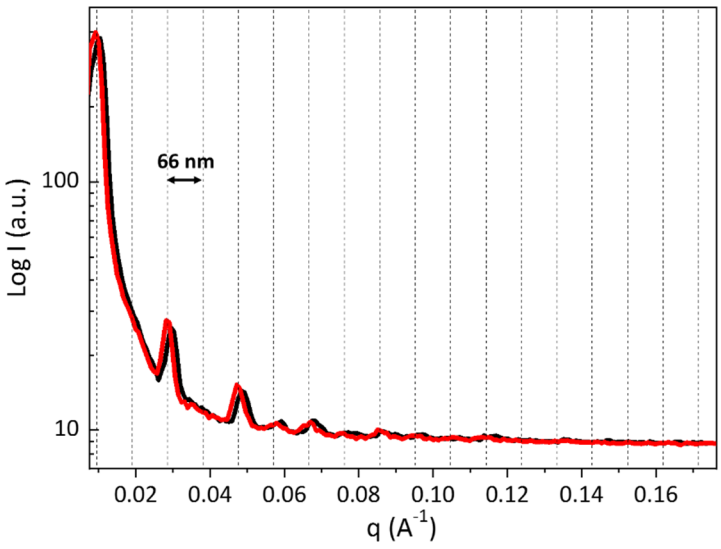

Figure 5. One-dimensional SAXS diffraction profiles obtained from radial integration of TG_4M_CTRL (black profile) and TG_4M_TRAT (red profile). The black dotted lines mark the periodicity along the fibril axis of ~65–66 nm ± 2 nm.

3.3. Differential Scanning Calorimetry Analysis

DSC is a powerful quantitative technique that provides a measure of protein (i.e., collagen) hydrothermal stability [30,31]. As known, type I collagen is the main constituent of fish skin [32], and it is a hierarchically organized protein characterized by an intimate relationship and connectivity among their individual structural levels [33]. Thermograms of skin samples from Tilapia fish fed with conventional and hydrolyzed collagen-supplemented feeding are all characterized by a single endothermic phenomenon (Figure 6) that could be ascribed to the skin's collagen content. As reported elsewhere, it is well known that a characteristic feature of collagen is the triple helical structure composed of three left-handed helices twisted into a right-handed superhelix by means of interchain hydrogen bonds [3,33]. While heating, the interchain hydrogen bonds of the right-handed superhelix break, and the triple helix unfolds in random chains [4]. Thus, the endothermal peak present within the temperature range of 0–100 °C, at about 65–67 °C, could be ascribed to the denaturation temperature (Td) of skin collagen. According to the literature, Td was found to be similar to that reported for the skin of land animals (i.e., pigs [34] and rats [35]). Unfortunately, to the best of our knowledge, few data were found on the DSC analysis on animal skin, and no data were found on Tilapia skin or other fish skin.

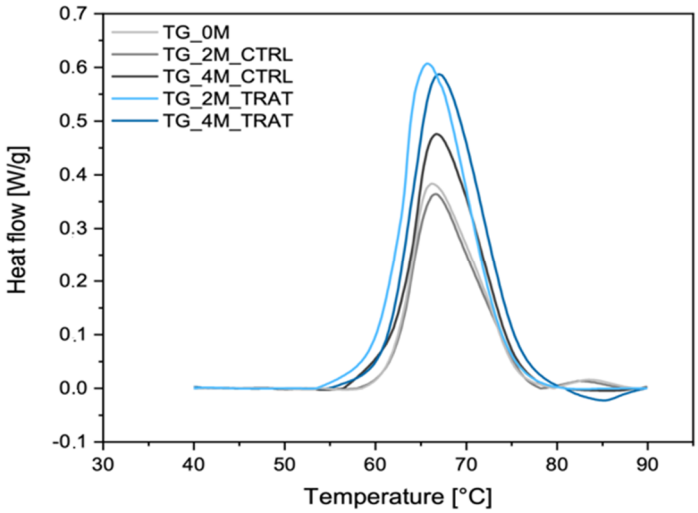

Figure 6. Representative thermograms of Tilapia skin from fish fed with conventional feed at time point 0 (TG_0M, light grey), two (TG_2M_CTRL, grey), and four months (TG_4M_CTRL, dark grey) and from fish fed a collagen-supplemented diet at two (TG_2M_TRAT, light blue) and four months (TG_4M_TRAT, blue).

Changes in the endothermic peak or enthalpy (ΔH) could be used to quantitatively assess the collagen structural variation in skin [4] (Table 2). Td was found to not be affected by fish age since it was discovered to be approximately the same in TG_0M (66.2 ± 0.4 °C), TG_2M_CTRL (66.6 ± 0.3 °C), and TG_4M_TRAT (66.5 ± 0.3) ($p > 0.05$). However, the effect of the enriched feeding could be detected as a reduction of the Td after two months of feeding (65.8 ± 0.3 °C) followed by its increase to slightly higher values after four months (67.3 ± 0.1 °C), compared to the control samples ($p < 0.05$).

While Td variations are slight, the energy absorption required for the transitions are significantly different. In CTRL samples, ΔH was found to increase from TG_0M (19.7 ± 1.5 J/g) to TG_4M_CTRL (27.9 ± 1.9 J/g). The fact that TG_4M_CTRL had a mean enthalpy value 1.4 times higher than TG_0M, indicated that at approximately the same value of Td, TG_4M_CTRL is more thermally stable than TG_0M because it requires more energy to carry out the thermal transition ($p < 0.05$). As regards ΔH values of Tilapia skin from fish fed a collagen-supplemented diet, it was found to be 1.6 times and 1.2 times higher than the Tilapia skin from fish fed with conventional feeding after two and four months, respectively. Although the increase in ΔH with respect to the control samples is significant,

there is no difference between the ΔH values of TG_2M_TRAT and TG_4M_TRAT. Thus, while the ΔH increase in the control samples could be ascribed to the increase in fish age, the ΔH increase in the treated samples could be an effect of the supplemented diet. In particular, the ΔH increase in collagen-fed fish could be due to the enriched diet, and it is associated with an increase in fish skin thermal stability.

Table 2. Mean values of the endothermic peak (Td) and enthalpy (ΔH) required for the endothermal transition that occurred on skin samples (n = 9, mean ± SD).

Sample	Td (°C)	ΔH (J/g)
TG_0M	66.2 ± 0.4	19.7 ± 1.5
TG_2M_CTRL	66.6 ± 0.3	21.6 ± 1.5
TG_2M_TRAT	65.8 ± 0.3	34.5 ± 3.0
TG_4M_CTRL	66.5 ± 0.3	27.9 ± 1.9
TG_4M_TRAT	67.3 ± 0.1	32.3 ± 2.1

Our results provide clear evidence that hydrolyzed collagen-supplemented feeding influences natural collagen organization in skin, probably by inducing the formation of more bonds between the collagen microfibrils or stimulating the biosynthesis of new collagen molecules.

4. Conclusions

The aim of the present work is to investigate the structural features of type I collagen when it is produced in Tilapia specimens grown with a collagen-supplemented diet. The aforementioned fish are a part of a circular system based on their being bred in an aquaponics plant and the use of the fish industry waste as a collagen source for biomedical, cosmetic, and nutraceutical applications. As already observed in the literature [13], the collagen's peptide supplementation can improve its deposition of collagen, in particular "coarse collagen", within skin. Thus, in this context, it was decided to add hydrolyzed collagen to the conventional feed to increase the yield of the protein from the fish. Wide- (WAXS) and small (SAXS)-angle X-ray scattering measurements performed on fish skin allowed us to inspect the collagen structure at both the sub and supramolecular scales, showing the length scale and parameter on which the supplementation acts. In particular, it was demonstrated that there was no effect of a collagen-rich diet at the molecular scale. On the other hand, the molecular arrangement of triple helices was affected by the animal age, contracting the molecular lateral packing. The helical pitch was preserved. Conversely, collagen-rich feed appears to increase the visibility of the fibrous matrix of the tissue. This hypothesis was supported by DSC data where the enthalpy required for the endothermal transition was found to be significantly higher for Tilapia fed with a hydrolyzed collagen-enriched diet. However, these tissues are no longer characterized by a fibrillary preferred orientation in the space, as the typical SAXS pattern is no longer visible. This could be due to an increased number of collagenous fibrils and dermal layers that are randomly oriented along the thickness of the dermis, the so-called "coarse collagen", already observed by Campos et al. [13].

Supplementary Materials: The following supporting information can be downloaded at: https://www.mdpi.com/article/10.3390/cryst12050700/s1, Figure S1: 2D WAXS diffraction patterns of Tilapia's skin from the control fish at time point 0 (TG_0M), two months (TG_2M_CTRL) and four months (TG_4M_CTRL) with conventional feed repeated over three different sets of materials.;. Figure S2: 2D WAXS diffraction patterns of Tilapia's skin from the control fish at time point 0 (TG_0M), two months (TG_2M_TRAT) and four months (TG_4M_TRAT) with with collagen nutritional supplementation over three different sets of materials. Figure S3: 2D WAXS pattern and the corresponding 1D profile acquired for on the Ultralene bag.

Author Contributions: Conceptualization, A.T., T.S., D.A. and C.G.; Data curation, A.T. and T.S.; Formal analysis, T.S., L.D.C. and C.G.; Investigation, A.T., T.S., N.G. and C.G.; Methodology, A.T., T.S., L.D.C., D.A. and C.G.; Resources, N.G., M.L.N., A.S., L.S., F.S.B. and A.C.; Software, L.D.C. and C.G.; Supervision, T.S. and C.G.; Writing—Original draft, A.T. and T.S.; Writing—Review and editing, L.D.C., D.A., N.G., A.S., L.S., M.L.N., F.S.B., A.C. and C.G. All authors have read and agreed to the published version of the manuscript.

Funding: This research was funded by the project "A system approach for identifying connective tissue degeneration in diabetic analogues—SAPIENT" Protocol Number: 2017CBHCWF and "ISEPA—Improving Sustainability, Efficiency and Profitability of Large-Scale Aquaponics (CUP: B37H17004760007)" by Regione Puglia in the framework of "InnoNetwork—Sostegno alle attivitaà di R&S per lo sviluppo di nuove tecnologie sostenibili, di nuovi prodotti e servizi".

Institutional Review Board Statement: Not applicable.

Informed Consent Statement: Not applicable.

Data Availability Statement: Not applicable.

Acknowledgments: R. Lassandro is acknowledged for his support in the XMI-Lab at CNR-IC.

Conflicts of Interest: The authors declare that the research was conducted in the absence of any commercial or financial relationships that could be construed as a potential conflict of interest.

References

1. Sorushanova, A.; Delgado, L.M.; Wu, Z.; Shologu, N.; Kshirsagar, A.; Raghunath, R.; Mullen, A.M.; Bayon, Y.; Pandit, A.; Raghunath, M.; et al. The Collagen Suprafamily: From Biosynthesis to Advanced Biomaterial Development. *Adv. Mater.* **2019**, *31*, 1801651. [CrossRef] [PubMed]
2. Ramachandran, G.N.; Kartha, G. Structure of Collagen. *Nature* **1955**, *176*, 593–595. [CrossRef] [PubMed]
3. Terzi, A.; Gallo, N.; Bettini, S.; Sibillano, T.; Altamura, D.; Madaghiele, M.; De, L.; Valli, L.; Salvatore, L.; Sannino, A.; et al. Sub- and Supramolecular X-ray Characterization of Engineered Tissues from Equine Tendon, Bovine Dermis, and Fish Skin Type-I Collagen. *Macromol. Biosci.* **2020**, *20*, 2000017. [CrossRef] [PubMed]
4. Salvatore, L.; Gallo, N.; Aiello, D.; Lunetti, P.; Barca, A.; Blasi, L.; Madaghiele, M.; Bettini, S.; Giancane, G.; Hasan, M.; et al. An insight on type I collagen from horse tendon for the manufacture of implantable devices. *Int. J. Biol. Macromol.* **2020**, *154*, 291–306. [CrossRef] [PubMed]
5. Zimmermann, E.A.; Gludovatz, B.; Schaible, E.; Dave, N.K.N.; Yang, W.; Meyers, M.A.; Ritchie, R.O. Mechanical adaptability of the Bouligand-type structure in natural dermal armour. *Nat. Commun.* **2013**, *4*, 2634. [CrossRef]
6. Gallo, N.; Natali, M.L.; Sannino, A.; Salvatore, L. An Overview of the Use of Equine Collagen as Emerging Material for Biomedical Applications. *J. Funct. Biomater.* **2020**, *11*, 79. [CrossRef]
7. Squire, J.M.; Freundlich, A. Direct observation of a transverse periodicity in collagen fibrils. *Nature* **1980**, *288*, 410–413. [CrossRef]
8. Silver, F.H.; Freeman, J.W.; Seehra, G.P. Collagen self-assembly and the development of tendon mechanical properties. *J. Biomech.* **2003**, *36*, 1529–1553. [CrossRef]
9. Li, W. Modelling methods for In Vitro biomechanical properties of the skin: A review. *Biomed. Eng. Lett.* **2015**, *5*, 241–250. [CrossRef]
10. Alberts, B.; Johnson, A.; Lewis, J.; Raff, M.; Roberts, K.; Walter, P. Molecular biology of the cell. 4th edn. *Ann. Bot.* **2003**, *91*, 401.
11. Salvatore, L.; Gallo, N.; Natali, M.L.; Campa, L.; Lunetti, P.; Madaghiele, M.; Blasi, F.S.; Corallo, A.; Capobianco, L.; Sannino, A. Marine collagen and its derivatives: Versatile and sustainable bio-resources for healthcare. *Mater. Sci. Eng. C* **2020**, *113*, 110963. [CrossRef] [PubMed]
12. Senaratne, L.S.; Park, P.J.; Kim, S.K. Isolation and characterization of collagen from brown backed toadfish (*Lagocephalus gloveri*) skin. *Bioresour. Technol.* **2006**, *97*, 191–197. [CrossRef] [PubMed]
13. Maia Campos, P.M.B.G.; Franco, R.S.B.; Kakuda, L.; Cadioli, G.F.; Costa, G.M.D.; Bouvret, E. Oral Supplementation with Hydrolyzed Fish Cartilage Improves the Morphological and Structural Characteristics of the Skin: A Double-Blind, Placebo-Controlled Clinical Study. *Molecules* **2021**, *26*, 4880. [CrossRef] [PubMed]
14. Czajka, A.; Kania, E.M.; Genovese, L.; Corbo, A.; Merone, G.; Luci, C.; Sibilla, S. Daily oral supplementation with collagen peptides combined with vitamins and other bioactive compounds improves skin elasticity and has a beneficial effect on joint and general wellbeing. *Nutr. Res.* **2018**, *57*, 97–108. [CrossRef]
15. Proksch, E.; Segger, D.; Degwert, J.; Schunck, M.; Zague, V.; Oesser, S. Oral supplementation of specific collagen peptides has beneficial effects on human skin physiology: A double-blind, placebo-controlled study. *Ski. Pharmacol. Physiol.* **2014**, *27*, 47–55. [CrossRef] [PubMed]
16. Maia Campos, P.M.B.G.; Melo, M.O.; Siqueira César, F.C. Topical application and oral supplementation of peptides in the improvement of skin viscoelasticity and density. *J. Cosmet. Derm.* **2019**, *18*, 1693–1699. [CrossRef]

17. Song, H.; Zhang, L.; Luo, Y.; Zhang, S.; Li, B. Effects of collagen peptides intake on skin ageing and platelet release in chronologically aged mice revealed by cytokine array analysis. *J. Cell Mol. Med.* **2018**, *22*, 277–288. [CrossRef]
18. Rinnerthaler, M.; Bischof, J.; Streubel, M.K.; Trost, A.; Richter, K. Oxidative stress in aging human skin. *Biomolecules* **2015**, *5*, 545. [CrossRef]
19. Altamura, D.; Lassandro, R.; Vittoria, F.; De Caro, L.; Siliqi, D.; Ladisa, M.; Giannini, C. X-ray microimaging laboratory (XMI-LAB). *J. Appl. Crystallogr.* **2012**, *45*, 899. [CrossRef]
20. Siliqi, D.; De Caro, L.; Ladisa, M.; Scattarella FMazzone, A.; Altamura, D.; Sibillano, T.; Giannini, C. SUNBIM: A package for X-ray imaging of nano- and biomaterials using SAXS, WAXS, GISAXS and GIWAXS techniques. *J. Appl. Crystallogr.* **2016**, *49*, 1107–1114. [CrossRef]
21. Salvatore, L.; Calò, E.; Bonfrate, V.; Pedone, D.; Gallo, N.; Natali, M.L.; Sannino, A.; Madaghiele, M. Exploring the effects of the crosslink density on the physicochemical properties of collagen-based scaffolds. *Polym. Test.* **2021**, *93*, 106966. [CrossRef]
22. Gallo, N.; Natali, M.L.; Curci, C.; Picerno, A.; Gallone, A.; Vulpi, M.; Vitarelli, A.; Ditonno, P.; Cascione, M.; Sallustio, F.; et al. Analysis of the Physico-Chemical, Mechanical and Biological Properties of Crosslinked Type-I Collagen from Horse Tendon: Towards the Development of Ideal Scaffolding Material for Urethral Regeneration. *Materials* **2021**, *14*, 7648. [CrossRef] [PubMed]
23. Elliott, D.G. THE SKIN | Functional morphology of the integumentary system in fishes. In *Encyclopedia of Fish Physiology*; Academic Press: Cambridge, MA, USA, 2011; pp. 476–488.
24. Bella, J.; Brodsky, B.; Berman, H.M. Hydratation structure of collagen peptide. *Structure* **1995**, *3*, 893–906. [CrossRef]
25. Bella, J. A new method for describing the helical conformation of collagen: Dependence of the tripe helical twist on amino acid sequence. *J. Struct. Biol.* **2010**, *170*, 377–391. [CrossRef]
26. Terzi, A.; Storelli, E.; Bettini, S.; Sibillano, T.; Altamura, D.; Salvatore, L.; Madaghiele, M.; Romano, A.; Siliqi, D.; Ladisa, M.; et al. Effects of processing on structural, mechanical and biological properties of collagen-based substrates for regenerative medicine. *Sci. Rep.* **2018**, *8*, 1429. [CrossRef]
27. Sibillano, T.; Terzi, A.; De Caro, L.; Ladisa, M.; Altamura, D.; Moliterni, A.; Lassandro, R.; Scattarella, F.; Siliqi, D.; Giannini, C. Wide Angle X-ray Scattering to Study the Atomic Structure of Polymeric Fibers. *Crystals* **2020**, *10*, 274. [CrossRef]
28. Terzi, A.; Gallo, N.; Bettini, S.; Sibillano, T.; Altamura, D.; Campa, L.; Natali, M.L.; Salvatore, L.; Madaghiele, M.; De Caro, L.; et al. Investigation of processing-induced structural changes in horse type-I collagen at sub and supramolecular levels. *Front. Bioeng. Biotechnol.* **2019**, *7*, 203. [CrossRef]
29. Rich, A.; Crick, F.H.C. The Molecular Structure of Collagen. *J. Mol. Biol.* **1971**, *3*, 483–506. [CrossRef]
30. Sun, L.; Hou, H.; Li, B.; Zhang, Y. Characterization of acid- and pepsin-soluble collagen extracted from the skin of Nile tilapia (Oreochromis niloticus). *Int. J. Biol. Macromol.* **2017**, *99*, 8–14. [CrossRef]
31. Rault, I.; Frei, V.; Herbage, D.; Abdul-Malak, N.; Huc, A. Evaluation of different chemical methods for cros-linking collagen gel, films and sponges. *J. Mater. Sci. Mater. Med.* **1996**, *7*, 215–221. [CrossRef]
32. Jafari, H.; Alberto Lista, A.; Manuela Mafosso Siekapen, M.M.; Pejman Ghaffari-Bohlouli, P.G.; Lei Nie, L.; Alimoradi, H.; Shavandi, A. Composition of Collagen Extracted from the Skin of Three Different Varieties of Fish. *Polymers* **2020**, *12*, 2230. [CrossRef] [PubMed]
33. Salvatore, L.; Gallo, N.; Natali, M.L.; Terzi, A.; Sannino, A.; Madaghiele, M. Mimicking the Hierarchical Organization of Natural Collagen: Toward the Development of Ideal Scaffolding Material for Tissue Regeneration. *Front. Bioeng. Biotechnol.* **2021**, *9*, 644595. [CrossRef] [PubMed]
34. Harrington, W.F.; Von Hippel, P.H. The Structure Of Collagen And Gelatin. *Adv. Protein Chem.* **1962**, *16*, 1–138.
35. Flandin, F.; Buffevant, C.; Herbage, D. A differential scanning calorimetry analysis of the age-related changes in the thermal stability of rat skin collagen. *Biochim. Et Biophys. Acta (BBA)-Protein Struct. Mol. Enzymol.* **1984**, *791*, 205–211. [CrossRef]